Turkish Journal of Chemistry

http://journals.tubitak.gov.tr/chem/

Research Article

Turk J Chem
(2016) 40: 602 – 612

doi:10.3906/kim-1509-28

Synthesis and computational studies of new metallo-phthalocyanines bearing dibenzoxanthenes and evaluation of their optical properties in solution and solid PMMA/ZnPc/Al nanocomposite films

Ali Reza KARIMI[1,*], Zeinab JAFARZADEH[1], Meysam SOURINIA[1], Akbar ZENDEHNAM[2], Azam KHODADADI[1], Zeinab DALIRNASAB[1], Mohammad SOLIMANNEJAD[1], Peyman ZOLGHARNEIN[3]

[1]Department of Chemistry, Faculty of Science, Arak University, Arak, Iran
[2]Department of Physics, Faculty of Science, Arak University, Arak, Iran
[3]Department of Materials Science and Engineering, Faculty of Engineering, Sheffield University, Sheffield, United Kingdom

Received: 13.09.2015 • **Accepted/Published Online:** 12.01.2016 • **Final Version:** 21.06.2016

Abstract: New thermally stable metallo-phthalocyanines bearing dibenzoxanthenes as highly organo-solubilizing aromatic hydrocarbon substituents were successfully prepared by cyclotetramerization of corresponding phthalonitriles with anhydrous metal salts [$Zn(CH_3COO)_2$ and $NiCl_2$] in the presence of a catalytic amount of DBU in 2-(dimethylamino) ethanol. All of these phthalocyanines are soluble in some organic solvents such as DMF, DMSO, THF, CH_2Cl_2, and $CHCl_3$. Then we successfully prepared the poly(methyl methacrylate) (PMMA)/ZnPc/Al nanocomposite films by incorporating Al nanoparticles into a transparent PMMA/ZnPc matrix. The structure and morphology of nanocomposite films were studied using X-ray diffraction and scanning electron microscopy. The optical absorption spectra of PMMA/ZnPc/Al nanocomposite films showed red shifting in the Q-band in the polymeric matrix. The geometrical structure of two phthalocyanines was investigated at the RHF/3-21G* computational level.

Key words: Soluble metallophthalocyanine, dibenzoxanthene, aggregation, nanocomposite film, geometry optimization

1. Introduction

For many years, phthalocyanines have been used as pigments.[1] Recently, Pc complexes have been investigated in diverse fields such as solar cells,[2] photovoltaic cells,[3] semiconductor devices,[4] electrochromic displays,[5] photodynamic therapy (PDT),[6,7] optical disks,[8] gas sensors,[9] chemical sensors,[10] liquid crystals,[11] film materials,[12] laser dye,[13] nonlinear optics,[14] and various catalytic processes.[15,16]

Stability and solubility are the main key factors to determine the functionality of a dye. Recently, synthesis of dye-based black matrix (BM), a component of LCD color filters, has been attracting extensive interest.[17,18] However, dyes as color filters are not widely used for commercial applications due to their unsatisfactory thermal stability and solubility. Therefore, the dyes for BM should have good solubility in industrial solvents and they need to be structurally stable.

Changing the substituents at the periphery of the benzene rings can significantly affect the physicochemical properties of phthalocyanine compounds.[19–25] This substitution gives flexibility in solubility and also

*Correspondence: a-karimi@araku.ac.ir

efficiently tunes the color of the phthalocyanines. Substitution of functional groups also changes the electron density of Pcs and finds use in various fields. The synthesis of xanthenes, especially benzoxanthenes, with biological and therapeutic properties such as antibacterial,[26] anti-inflammatory,[27] and antiviral[28] has attracted significant interest. Furthermore, these heterocyclic compounds are used as sensitizers in photodynamic therapy[29] and antagonists for the paralyzing action of zoxazolamine.[30] Moreover, due to their useful spectroscopic properties, they are used as dyes,[31] in laser technologies,[32] and in fluorescent materials for visualization of biomolecules.[33]

Encouraged by this information and due to our interest in the synthesis of Pcs,[34–36] herein we report the preparation of new phthalocyanines (Pcs) containing four dibenzoxanthene groups as substituents on the zinc phthalocyanine structure to increase the solubility of the studied Pcs (Scheme).

Then we prepared the PMMA/ZnPc/Al nanocomposite films by incorporating Al nanoparticles into a transparent PMMA/ZnPc matrix. Zinc-phthalocyanine (Zn-Pc) in a polymeric matrix was amplified with various loadings (5%, 10%, and 15%) of aluminum.

Optical properties of thermally stable metallo-phthalocyanines bearing dibenzoxanthenes in solution and solid PMMA nanocomposite films have been investigated. The PMMA/ZnPc/Al nanocomposite films exhibit a red shift effect in Q-band absorption of phthalocyanine.

2. Results and discussion

Phthalonitrile derivatives **5a**, **5b**, and **5c** were synthesized in two steps (Scheme). First, dicyano compounds **3a**–**c** were obtained by nucleophilic aromatic nitro displacement on 4-nitrophthalonitrile **1** with hydroxybenzaldehydes **2a**–**c** in the presence of anhydrous K_2CO_3 as the base in DMF. Then compounds **3a**–**c** were reacted with two equivalents of β-naphthol under solvent-free conditions in the presence of p-toluene sulfonic acid as the catalyst.[37] Compounds **3a**–**c** were obtained in 90%, 84%, and 81% yields, respectively. The IR spectra of **5a**, **5b**, and **5c** clearly indicate the presence of CN vibrational peaks at 2236, 2231, and 2231 cm^{-1}, respectively. The ^1H NMR spectra were also in good agreement with the structures of the compounds **5a**, **5b**, and **5c**. For instance, the spectrum of **5a** exhibited an aliphatic proton as a singlet at δ 6.55 ppm (1H). The aromatic protons in the low field region appear as two doublets at δ 6.83 (2H) and 7.03 ppm (1H), a singlet at δ 7.16 ppm (1H), a multiplet at δ 7.47–7.89 ppm (13H), and a doublet at δ 8.37 ppm (2H).

The metallophthalocyanines **6**–**10** were obtained by cyclotetramerization of dinitrile compounds **5a**, **5b**, and **5c** (3 mmol) in the presence of anhydrous metal salts [$NiCl_2$ and $Zn(CH_3COO)_2$] (1 mmol) using DBU as catalyst. The reaction was carried out in refluxing 2-(dimethylamino)ethanol (DMAE) under a nitrogen atmosphere. IR, ^1H NMR, MALDI-TOF-MS, and UV-vis spectra confirmed the proposed structures of the synthesized metallophthalocyanines. Thermogravimetric analysis (TGA) was used for determining the thermal stability of these complexes. The IR spectra of phthalocyanines **6**–**10** lacked the CN band completely. The IR spectra of nanocomposite films showed new peaks attributed to the PMMA matrix. The ^1H NMR spectrum of **7** indicated aromatic protons as multiplets at δ 6.82–8.38 ppm. The aliphatic CH protons appeared at δ 6.55 ppm. In the ^1H NMR spectrum of **8**, the aliphatic CH_3 group protons appeared at δ 3.57 ppm, protons of CH groups appeared at δ 6.57 ppm, and aromatic protons were observed as a multiplet at δ 7.05–8.43 ppm. The MALDI–TOF–MS measurement for compounds **7**, **8**, and **10** gave the characteristic molecular ion peaks at m/z: 2061, 2188, and 2067 [M^+], respectively, confirming the proposed structures.

The thermal behavior of phthalocyanines **7**, **8**, and **10** was analyzed by TGA in the temperature range

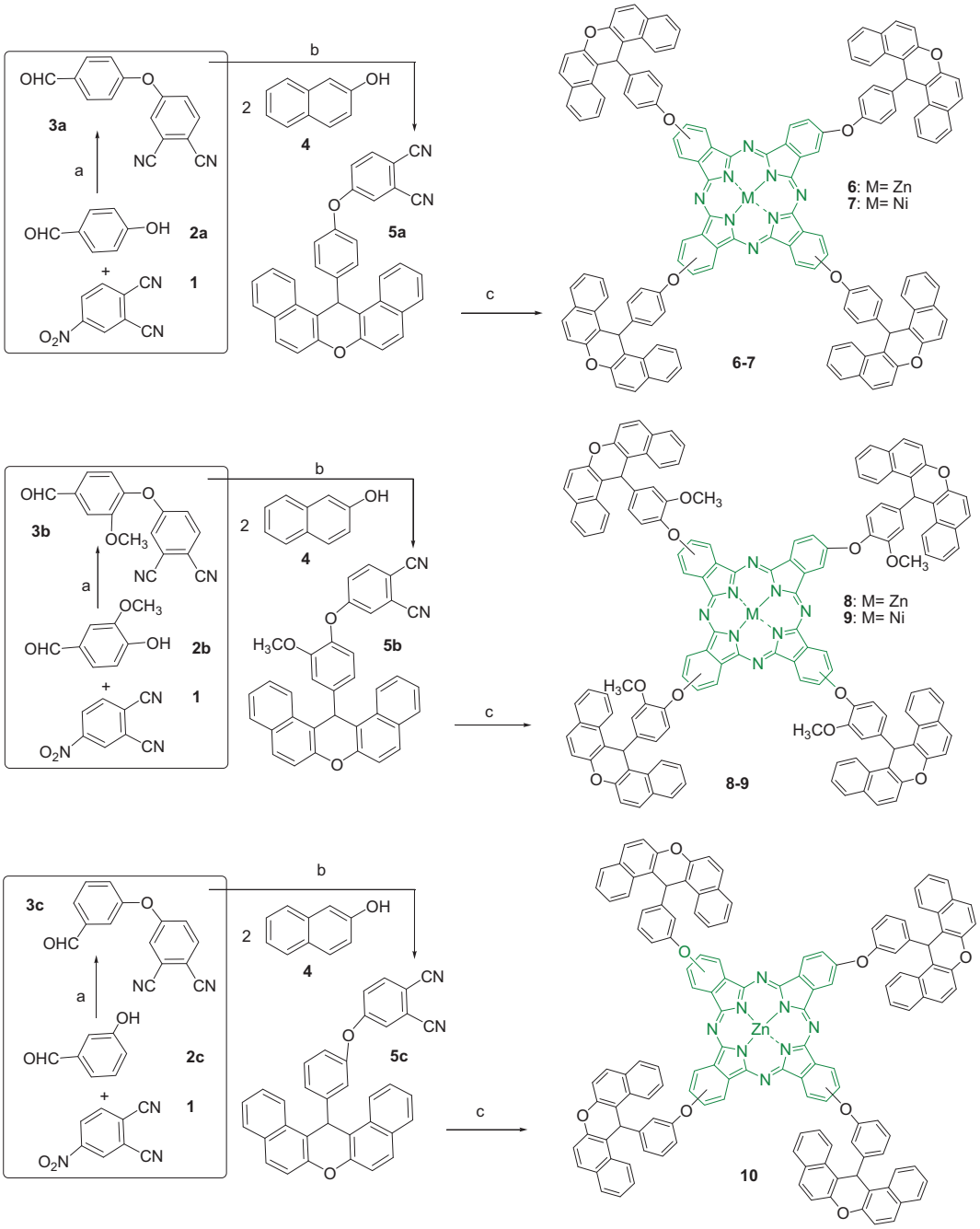

Scheme. Synthesis of metallophthalocyanines **6**–**10**. Reagents and conditions: (a) K_2CO_3, DMF, 24 h, rt; (b) Solvent-free, *p*-TSA, 125 °C, 20 min; (c) $Zn(OAc)_2$ or $NiCl_2$, DBU, DMAE, N_2, reflux 18 h. 6: 34%, 7: 36%, 8: 35%, 9: 41%, 10: 33%.

30–1000 °C under a nitrogen atmosphere with a heating rate of 10 °C/min. The first weight loss below 120 °C is related to vaporization of trapped solvent such as water or ethanol. Significant loss of weight started after 320 °C. This loss was attributed to a major decomposition reaction between 320 and 800 °C. These results are summarized in Table 1. The loss of weight at 800 °C was 37% for **7**, 55% for **8**, and 40% for **10**.

Table 1. Thermal analyses data for **7**, **8**, **10**.

Name	Mass loss (up to 300 °C)	Mass loss (up to 800 °C)
7	3%	37%
8	5%	55%
10	3%	40%

The structure and morphology of PMMA/ZnPc/Al nanocomposite films were studied using X-ray diffraction (XRD) and scanning electron microscopy (SEM). A SEM image of one of the nanocomposite films is shown in Figure 1. This image exhibited a uniform distribution of aluminum nanoparticles in the polymer matrix. There it can be seen that the average size of nanocomposite film containing 10% aluminum is 29.8 nm.

XRD patterns of the PMMA/ZnPc/Al nanocomposite films showed four peaks for Al at 38.583°, 44.848°, 65.220°, and 78.352° (Figure 2). Moreover, XRD of nanocomposite films shows two peaks at 2θ: 15° and 20° that are attributed to the polymeric matrix (Figure 2). The particle size of crystalline aluminum was determined from XRD details by the Debye–Scherrer equation. The results revealed that the particle size was less than 100 nm.

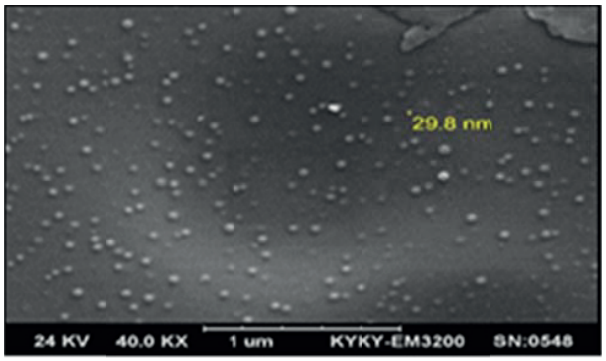

Figure 1. Scanning electron microscopy image. PMMA (0.2 g)/ZnPc **6** (0.01 g)/Al (10%).

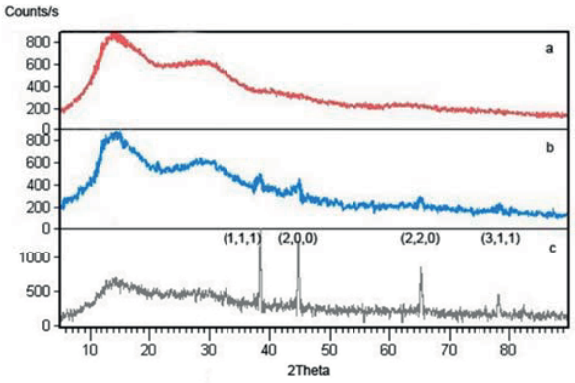

Figure 2. XRD spectra of (a) PMMA (0.2 g)/ZnPc **6** (0.01 g); (b) PMMA (0.2 g)/ZnPc **6** (0.01 g)/Al (10%); (c) PMMA (0.2 g)/ZnPc **6** (0.01 g)/Al (15%).

Furthermore, the surface roughness of nanocomposite films was measured. The results of surface roughness of nanocomposite films are shown in Figure 3 and Table 2. These results indicate the accumulation of nanoparticles in the nanocomposite films has not been observed and the high percentage of Al nanoparticles leads to an increase in the roughness of nanocomposite films.

Table 2. The surface roughness of nanocomposite films.

Name	Ra (μm)	Rq (μm)	Rv (μm)
a	0/240	0/300	0/615
b	0/402	0/402	0/664
c	1/219	1/610	2/927

(a) PMMA (0.2 g)/ZnPc **6** (0.01 g)/ Al (5%); (b) PMMA (0.2 g)/ZnPc **6** (0.01 g)/Al (10%); (c) PMMA (0.2 g)/ZnPc **6** (0.01 g)/Al (15%).

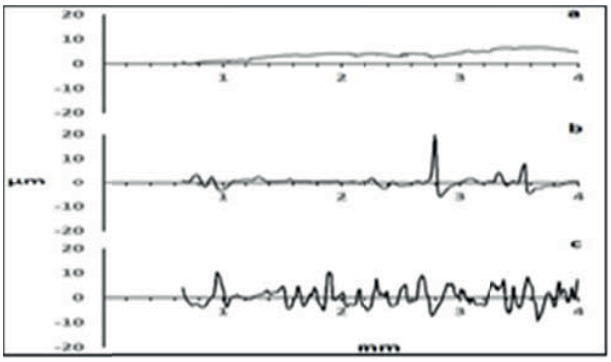

Figure 3. The results of surface roughness of nanocomposite films. PMMA (0.2 g)/ZnPc **6** (0.01 g)/(a) Al (5%); (b) Al (10%); (c) Al (15%).

Moreover, optical microscopy (OM) images of nanocomposite films are shown in Figures 4a and 4b. Observation of solid surface nanocomposites in an optical microscope can result in some qualitative information about dispersion. These images showed that the dispersion in nanocomposite film containing 10% Al is better than that in other nanocomposites.

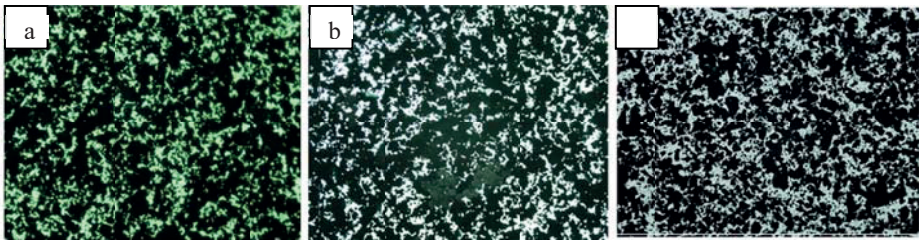

Figure 4. Optical microscopy image of nanocomposite films of (a) PMMA (0.2 g)/ZnPc **6** (0.01 g)/Al (5%); (b) PMMA (0.2 g)/ZnPc **6** (0.01 g)/Al (10%); (c) PMMA (0.2 g)/ZnPc **6** (0.01 g)/Al (15%).

The UV-vis spectra of the phthalocyanines **6**–**10** in DMF are shown in Figure 5. The UV spectra of the phthalocyanines **6**–**10** show single intense bands at λ_{max} = 681, 677, 683, 673, and 682 nm, respectively. There is also a shoulder-like absorption at slightly higher energy for all the phthalocyanines. The weaker absorptions appear at 613, 614, 615, 606, and 614 nm for phthalocyanines **6**–**10**, respectively. This is typical of metal complexes of substituted and unsubstituted metallophthalocyanines with D_4h symmetry.[38] The B bands for **6**–**10** were observed at 334, 333, 350, 333, and 356 nm, respectively (Figure 5; Table 3).

Table 3. Absorption data for phthalocyanines **6**–**10** in DMF (c = 3 × 10^{-5} M).

Pc	λ_{max} (nm) (log ε)
6	681 (3.83), 613 (3.23), 334 (4.66)
7	677 (4.45), 613 (3.98), 333 (4.26)
8	683 (4.97), 615 (4.33), 350 (4.85)
9	673 (4.84), 606 (4.29), 333 (4.56)
10	682 (4.57), 614 (3.85), 356 (4.28)

Phthalocyanines **6**–**10** are soluble in THF, CH_2Cl_2, CH_3Cl, DMSO, and DMF. In the solid state, the absorption spectra for thin films (Figure 6) are different from their solution spectra in which the Q-band looks

like very sharp. The optical absorption spectra of PMMA/Zn-Pc nanocomposite films for compound **6** shown in Figure 6 and Table 4 indicate red shifting in the Q-band.

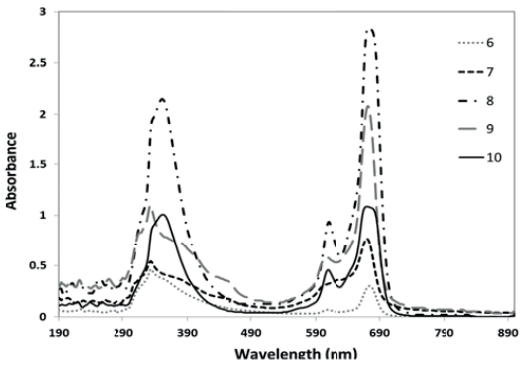

Figure 5. Absorption spectra of **6**–**10** in DMF (c = 3 × 10^{-5} M).

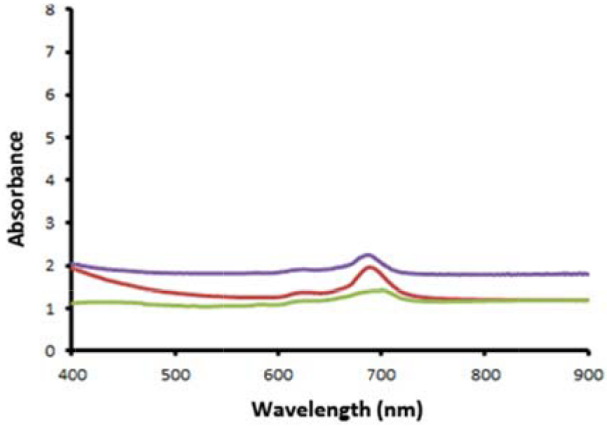

Figure 6. Absorption spectra of phthalocyanine **6** in nanocomposite films (a) PMMA (0.2 g)/ZnPc **6** (0.01 g)/ Al (5%); (b) PMMA (0.2 g)/ZnPc **6** (0.01 g)/Al (10%); (c) PMMA (0.2 g)/ZnPc **6** (0.01 g)/Al (15%).

Table 4. Absorption data for phthalocyanine **6** in nanocomposite films.

PMMA/ZnPc/Al	λ_{max} Q-band (nm)	Al%
a	685	5
b	700	10
c	686	15

PMMA (0.2 g), ZnPc (0.01 g).

The absorption spectra of PMMA/ZnPc/Al nanocomposite films shown clearly demonstrate the absorption peaks at 600–700 nm corresponding to the Q-bands of phthalocyanine. When compared with the UV/vis absorption spectrum of ZnPc **6** in DMF, whose main absorption bands are located at 681 and 613 (Q-band) and 334 nm (B-band), respectively, formation of PMMA/ZnPc/Al nanocomposite films leads to a red shift of the Q-band.

Aggregation is usually depicted as a coplanar association and is dependent on the nature of solvent, concentration, nature of substituent, center metal ions, and temperature.[39] In the present study the aggregation behavior of complexes was investigated at different concentration and different solvents. The aggregation behaviors of phthalocyanines **6**–**10** at three concentrations (5 × 10^{-5}, 4 × 10^{-5}, 3 × 10^{-5} M) in DMSO, DMF, CH_3Cl, and THF were considered. The intensity of the absorption bands was increased with increasing concentration and there were no new bands due to the aggregated species. Thus phthalocyanines **6**–**10** did not show aggregation in these solvents at different concentrations. For example, phthalocyanine **6** did not show aggregation in DMSO. The Lambert–Beer law was obeyed for phthalocyanine **6** as an example in the concentrations ranging from 5 × 10^{-5} to 3 × 10^{-5} M in DMSO (Figure 7).

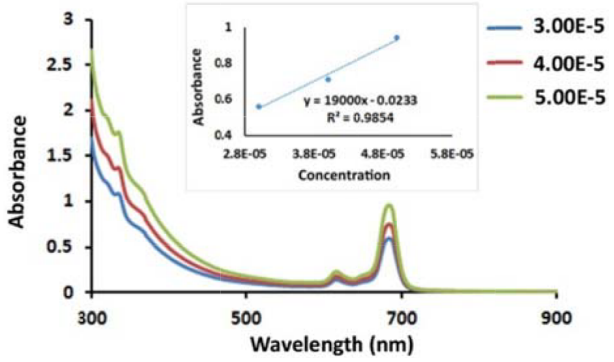

Figure 7. Absorption spectra of **6** in DMSO in different concentrations.

Calculations were performed with the Gaussian 03[40] system of codes at the restricted Hartree–Fock level of theory with the 3-21G* basis set.[41] The total energies and relative energy of the optimized structures and dipole moments calculated at HF are presented in Table 5. The results of calculations show that phthalocyanine **6** is more stable than phthalocyanine **10** in the gas phase but the dipole moment of **10** is more than that of phthalocyanine **6**. The optimized molecular structures of phthalocyanines **6** and **10** are shown in Figure 8.

Table 5. The total energy, ratio of energy, dipole moment of **6** and **10** calculated by HF/3-21 G* method.

Pc	energy[a]	μ^{b}_{tota}
6	–8116.54216342	4.7580
10	–8116.54080792	7.6970

[a] Total energy in hartree units. [b] Total dipole moment in debyes.

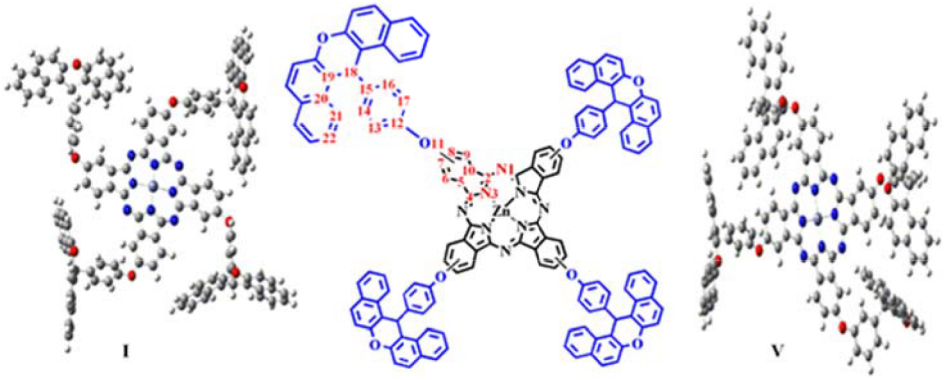

Figure 8. Optimized geometries of **6** and **10**.

The comparative optimized structural parameters such as bond lengths, bond angles, and dihedral angle values for phthalocyanines **6** and **10** are presented in Table 6. The N1–C2, N3–C4, C4–C5, C2–C10, O11–C12, C15–C18, and C18–C19 bond lengths were increased but for C7–O11 a reduction in bond length was obtained. The optimized structure may be compared with the other structures.

3. Experimental

3.1. General

Synthesis of 4-(4-formylphenoxy)phthalonitrile (**3a**): A mixture of 4-nitrophthalonitrile **1** (1 mmol), 4-hydroxybenzaldehyde **2a** (1 mmol), and K_2CO_3 (1 mmol) was dissolved in 2 mL of DMF. The mixture was stirred at

room temperature for 24 h. After completion of the reaction, 5 mL of acetone and 4 mL of water were added consecutively to the reaction mixture and the resulting precipitates were separated and washed with 10 mL of hot water and 10 mL of ethanol. Yield: 90%, mp: 154 °C. IR υ_{max}/cm^{-1} (KBr pellet): 3103, 3078 (CH_{arom}), 2850, 2760 ($C–H_{aldehyde}$), 2236 (C≡N), 1691 (C=O), 1589 (C=C), 1087 (C–O).[35]

Table 6. Selected optimized bond lengths (Å), bond angles (°C), and dihedral angles (°C) of **6** and **10**.

Pc	Bond lengths	Å	Bond angle	°C	Dihedral angle	°C
6	N1–C2	1.28	N1–C2–N3	126.58	N1–C2–C10–C9	0.6649
	N3–C4	1.33	N3–C4–C5	109.85	C7–O11–C12–C13	–85.16
	C4–C5	1.46	N3–C2–C10	107.49	C7–O11–C12–C17	101.11
	C2–C10	1.46	C2–C10–C9	131.56	C14–C15–C18–C19	–61.24
	C7–O11	1.39	C4–C5–C6	132.22	C19–C20–C21–C22	179.45
	O11–C12	1.39	C7–O11–C12	122.43		
	C15–C18	1.53	C15–C18–C19	109.75		
	C18–C19	1.43	C18–C19–C20	122.27		
			C19–C20–C21	122.98		
10	N1–C2	1.29	N1–C2–N3	126.25	N1–C2–C10–C9	0.8386
	N3–C4	1.36	N3–C4–C5	108.83	C7–O11–C13–C14	31.44
	C4–C5	1.47	N3–C2–C10	109.15	C7–O11–C13–C12	136.70
	C2–C10	1.47	C2–C10–C9	132.62	C14–C15–CC18–C19	119.62
	C7–O11	1.38	C4–C5–C6	132.58	C19–C20–C21–C22	179.67
	O11–C13	1.40	C7–O11–C13	129.80		
	C15–C18	1.53	C15–C18–C19	111.05		
	C18–C19	1.53	C18–C19–C20	121.81		
			C19–C20–C21	122.88		

Synthesis of (4-(14H-dibenzo[a,j]xanthen-14-yl)phenoxy)phthalonitriles (**5a**–**c**): Phthalonitriles **5a**–**c** were prepared according to our published procedure.[42]

Synthesis of 2, 9, 16, 23-tetrakis(4-(14H-dibenzo[a,j]xanthen-14-yl)phenoxy)zinc(II) phthalocyanine (**6**): A mixture of compound **5a** (0.15 g, 0.3 mmol), anhydrous $Zn(OAc)_2$ (0.019 g, 0.1 mmol), DBU (3 drops), and DMAE (10 mL) was refluxed under nitrogen atmosphere for 18 h. The reaction mixture was then cooled to room temperature. In the next step ethanol was added and the product was filtered under reduced pressure. The green solid was washed several times with hot ethanol. This compound was soluble in DMSO, THF, CH_3Cl, CH_2Cl_2, and DMF. IR υ_{max}/cm^{-1} (KBr pellet): 3057 (CH_{arom}), 1616 (C=N), 1593 (C=C), 1170, 1087 (C–O).; ^{1}H NMR (300 MHz, DMSO-d_6) δ_H: 6.76 (s, 4H, CH), 6.88–7.12 (m, 16H, Ar–H), 7.15–7.65 (m, 32H, Ar-H), 7.85–7.95 (m, 20H, Ar–H), 8.65–8.75 (m, 8H, Ar–H). (MALDI–TOF) m/z: 2067.57 [M^+]. Elemental analysis: calcd (%) for $C_{140}H_{80}N_8O_8Zn$, C 81.59, H 3.91, N 5.44; found, C 81.25, H 4.02, N 5.31.

Synthesis of 2, 9, 16, 23-tetrakis(4-(14H-dibenzo[a,j]xanthen-14-yl)phenoxy)nickel(II) phthalocyanine (**7**): A mixture of compound **5a** (0.15 g, 0.3 mmol), $NiCl_2$ (0.013 g, 0.1 mmol), three drops of DBU, and DMAE (7 mL) was refluxed at 130 °C under nitrogen atmosphere for 18 h. After cooling to room temperature the mixture was treated with EtOH (2 mL) in order to precipitate the product. The precipitated dark green product was filtered off and washed with 10 mL of hot ethanol and 10 mL of hot water. Yield: 38%. IR υ_{max}/cm^{-1} (KBr pellet): 3055 (CH_{arom}), 1618 (C=N), 1593, 1502 (C=C), 1165, 1091 (C–O). MS (MALDI–TOF) m/z: 2060.88

[M^+]. Elemental analysis: calcd (%) for $C_{140}H_{80}N_8O_8Ni$, C 81.59, H 3.91, N 5.44; found, C 80.95, H 5.25, N 5.61.

Synthesis of 2, 9, 16, 23-tetrakis(4-(14H-dibenzo[a,j]xanthen-14-yl)-2-methoxyphenoxy)zinc (II) phthalocyanine (**8**): The zinc(II) phthalocyanine **8** prepared as described for **6** using compound **5b** (0.16 g, 0.3 mmol), anhydrous $Zn(OAc)_2$ (0.019 g, 0.1 mmol), and DBU (3 drops) in 10 mL of DMAE. This compound was soluble in DMSO, THF, CH_3Cl, CH_2Cl_2, and DMF. IR υ_{max}/cm^{-1} (KBr pellet): 3045 (CH_{arom}), 1616 (C=N), 1593, 1506 (C=C), 1124, 1087 (C–O); ^{1}H NMR (300 MHz, $CDCl_3$) δ_H: 3.57 (s, 12H), 6.56 (s, 4H), 6.87–7.91 (m, 64H, Ar–H), 8.41 (d, J = 9.0 Hz, 8H, Ar–H). MS (MALDI–TOF) m/z: 2188 [M^+]. Elemental analysis: calcd (%) for $C_{144}H_{88}N_8O_{12}Zn$, C 79.30, H 4.07, N 5.14; found, C 78.25, H 4.25, N 5.21.

Synthesis of 2, 9, 16, 23-tetrakis(4-(14H-dibenzo[a,j]xanthen-14-yl)-2-methoxyphenoxy)phthalocyanine nickel(II) phthalocyanine (**9**): A mixture of compound **5b** (0.16 g, 0.3 mmol), $NiCl_2$ (0.013 g, 0.1 mmol), three drops of DBU, and DMAE (7 mL) was refluxed at 130 °C under nitrogen atmosphere for 18 h. After cooling to room temperature the mixture was treated with EtOH (2 mL) in order to precipitate the product. The precipitated dark green product was filtered off and washed with 10 mL of hot ethanol and 10 mL of hot water. Yield: 41%. IR υ_{max}/cm^{-1} (KBr pellet): 3031 (CH_{arom}), 1618 (C=N), 1593, 1506 (C=C), 1124, 1093 (C–O); ^{1}H NMR (300 MHz, $CDCl_3$) δ_H: 3.59 (s, 12H, CH_3), 5.59 (s, 4H, CH), 6.90–6.94 (m, 8H, Ar–H), 7.07–7.13 (m, 8H, Ar–H), 7.21–7.56 (m, 20H, Ar–H), 7.63–7.69 (m, 12H, Ar–H), 7.87–7.93 (m, 16H, Ar–H), 8.42 (d, J = 9 Hz, 8H, Ar–H). MS (MALDI–TOF) m/z: 2180.98 [M^+]. Elemental analysis: calcd (%) for $C_{144}H_{88}N_8O_{12}Ni$, C 79.30, H 4.07, N 5.14; found, C 79.28, H 4.00, N 5.01.

Synthesis of 2, 9, 16, 23-tetrakis(3-(14H-dibenzo[a,j]xanthen-14-yl)phenoxy)zinc(II) phthalocyanine (**10**): A mixture of compound **5c** (0.15 g, 0.3 mmol), $Zn(OAc)_2$ (0.019 g, 0.1 mmol), three drops of DBU, and DMAE (7 mL) was refluxed at 130 °C under nitrogen atmosphere for 18 h. After cooling to room temperature the mixture was treated with EtOH (2 mL) in order to precipitate the product. The precipitated dark green product was filtered off and washed with 10 mL of hot ethanol and 10 mL of hot water. Yield: 35%. IR υ_{max}/cm^{-1} (KBr pellet): 3081 (CH_{arom}), 1618 (C=N), 1593, 1506 (C=C), 1124, 1093 (C–O); ^{1}H NMR (300 MHz, $CDCl_3$) δ_H: 6.51–6.73 (m, 8H, Ar–H), 6.93–7.18 (m, 8H, Ar–H), 7.29–7.60 (m, 28H, Ar–H), 7.61–7.69 (m, 20H, Ar–H), 7.80–7.83 (m, 8H, Ar–H), 8.34–8.43 (m, 8H, Ar–H). MS (MALDI–TOF) m/z: 2067 [M^+]. Elemental analysis: calcd (%) for $C_{140}H_{80}N_8O_8Zn$, C 81.59, H 3.91, N 5.44; found, C 82.00, H 3.98, N 5.12.

Preparation of PMMA/ZnPc film and PMMA/ZnPc/Al nanocomposite films: For the fabrication of the ZnPc/nanocomposite films, 0.01 g of phthalocyanine **6** was dissolved in 1 mL of DMF. The solution was stirred at 100 °C for 2 h. Then a solution of 0.2 g of PMMA in 3 mL of DMF was prepared. Both solutions were mixed together and homogenized by magnetic agitation for 24 h at room temperature. Then the solution was mixed with three different amounts (0.01, 0.02, and 0.03 g) of aluminum nanoparticles under ultrasound irradiation for 2 h. Nanocomposite films were cast by pouring the solutions of each concentration into petri dishes placed on a leveled surface followed by evaporation of the solvent at 70 °C over 12 h. The films were dried at 80 °C for 24 h under vacuum to a constant weight. The mixture was poured in petri dishes and placed on a leveled surface.

4. Conclusion

Tetra-substituted metallophthalocyanines **6**–**10** bearing dibenzoxanthenes have been synthesized for the first time in good yield. These complexes have been characterized on the basis of their elemental analysis and by

UV-vis, FT-IR, ^{1}H NMR, and MALDI–TOF mass spectroscopies and thermogravimetric analysis. Moreover, metallophthalocyanine **6** has been incorporated into polymer PMMA host and nanocomposite films by varying the amounts of Al from 5% to 15% were synthesized. The obtained solid nanocomposites exhibit red shifting in the Q-band. Among the produced nanocomposite thin films, nanocomposite film containing 10% Al showed the most red shift in Q-band absorption. The structure and morphology of PMMA/ZnPc/Al nanocomposite films were studied using XRD, SEM, and OM. The average size of nanocomposite film containing 10% Al was 29.8 nm. Geometry optimization of two complexes at RH/3-21G* computational level gives more insights regarding structural parameters in studied complexes.

Acknowledgment

We gratefully acknowledge the financial support from the Research Council of Arak University.

References

1. Leznoff, C. C.; Lever, A. B. P. Eds. *Phthalocyanines Properties and Applications*, Vol. 1–3, VCH: New York, NY, USA, 1989–1993.
2. Takahashi, K.; Kuraya, N.; Yamaguchi, T.; Komura, T.; Murata, K. *Sol. Energ. Mater. Sol. Cell.* **2000**, *61*, 403-416.
3. Kikuchi, E.; Kitada, S.; Ohno, A.; Aramaki, S.; Maenosono, S. *Appl. Phys. Lett.* **2008**, *92*, 173307-173309.
4. Cai, X.; Zhang, Y.; Qi, D.; Jiang, J. *J. Phys. Chem. A.* **2009**, *113*, 2500-2506.
5. Somani, P. R.; Radhakrishnan, S. *Mater. Chem. Phys.* **2002**, *77*, 117-133.
6. Herlambang, S.; Kumagai, M.; Nomoto, T.; Horie, S.; Fukushima, S.; Oba, M.; Miyazaki, K.; Morimoto, Y.; Nishiyama, N.; Kataoka, K. *J. Control Release* **2011**, *155*, 449-457.
7. Yılmaz, Y.; Erdoğmuş, A.; Şener, M. K. *Turk. J. Chem.* **2014**, *38*, 1083-1093.
8. Zhang, W.; Ishimaru, A.; Onouchi, H.; Rai, R.; Saxena, A.; Ohira, A.; Ishikawa, M. Naito, M.; Fujiki, M. *New J. Chem.* **2010**, *34*, 2310-2018.
9. Collins, G. E.; Armstrong, N. R.; Pankow, J. W.; Oden, C.; Brina, R.; Anbour, C.; Dodelet, J. P.; Vac. J. *Sci. Technol. A.* **1993**, *11*, 1383-1391.
10. Zhang, Y. J.; Hu, W. P. *Sci. China Ser. B* **2009**, *52*, 751-754.
11. Nyokong, T. *Struct. Bond.* **2010**, *135*, 45-88.
12. Srinivasan, M. P.; Gu, Y.; Begum, R. *Coll. Surf. A*, **2002**, *198*, 527-534.
13. Leznoff, C. C.; Lever, A. B. P. Eds. In *Phthalocyanines, Properties and Applications*; Vol. 4, VCH: New York, NY, USA: 1996, pp. 219-284.
14. De La Torre, G.; Vazquez, P.; Agullo-Lopez, F.; Torres, T. *J. Mater. Chem.* **1998**, *8*, 1671-1683.
15. Shinu, V. S.; Pramitha, P.; Bahulayan, D. *Tetrahedron Lett.* **2011**, *52*, 3110-3115.
16. Saka, E.; Bıyıklıoğlu, Z.; Kantekin, H. *Turk. J. Chem.* **2014**, *38*, 1166-1173.
17. Lee, W.; Yuk, S. B.; Choi, J.; Jung, D. H.; Choi, S. H.; Park, J.; Kim, J. P. *Dyes Pigments* **2012**, *92*, 942-948.
18. Kim, Y. D.; Kim, J. P.; Kwon, O. S.; Cho, I. H. *Dyes Pigments* **2009**, *81*, 45-52.
19. Karaca, H.; Sezer, S.; Tanyeli, C. *Dyes Pigments* **2011**, *90*, 100-105.
20. Kluson, P.; Drobek, M.; Kalaji, A.; Karaskova, M.; Rakusan, J. *Res. Chem. Intermediat.* **2009**, *35*, 103-116.
21. Booysen, I.; Matemadombo, F.; Durmus, M.; Nyokong, T. *Dyes Pigments* **2011**, *89*, 111-119.
22. Lokesh, K. S.; Adriaens, A. *Dyes Pigments* **2013**, *96*, 269-277.
23. Gök, H. Z.; Farsak, B.; Keleş, H.; Keleş, M. *Turk. J. Chem.* **2014**, *38*, 1073-1082.

24. Özçeşmeci, M.; Nar, I.; Hamuryudan, E. *Turk. J. Chem.* **2014**, *38*, 1064-1072.
25. Kartaloğlu, N.; Esenpınar, A. A.; Bulut, M. *Turk. J. Chem.* **2014**, *38*, 1102-1117.
26. Hideo, T. *Chem. Abstr.* **1981**, *95*, 80922b.
27. Poupelin, J. P.; Saint-Rut, G.; Foussard-Blanpin, O.; Narcisse, G.; Uchida-Ernouf, G.; Lacroix, R. *Eur. J. Med. Chem.* **1978**, *13,* 67-71.
28. Lambert, R. W.; Martin, J. A.; Merrett, J. H.; Parkes, K. E. B.; Thomas, G J. J. *Chem. Abstr.* **1997**, 126, p212377y.
29. Ion, R. M.; Frackowiak, D.; Planner, A.; Wiktorowicz, K. *Acta Biochim. Pol.* **1998**, *45*, 833-845.
30. Saint-Ruf, G.; De, A.; Hieu, H. T. *Bull. Chim. Ther.* **1972**, *7*, 83-86.
31. Menchen, S. M.; Benson, S. C.; Lam, J. Y. L.; Zhen, W.; Sun, D.; Rosenblum, B. B.; Khan, S. H.; Taing, M. *U.S. Patent* **2003**, 6583168, *Chem. Abstr.* **2003**, *139*, 54287f.
32. Ahmad, M.; King, T. A.; Ko, Do-K.; Cha, B. H.; Lee, J. *J. Phys. D: Appl. Phys.* **2002**, *35*, 1473-1476.
33. Knight, C. G.; Stephens, T. *Biochem. J.* **1989**, *258*, 683-687.
34. Karimi, A. R.; Bayat, F. *Tetrahedron Lett.* **2012**, *53*, 123-126.
35. Karimi, A. R.; Khodadadi, A. *Tetrahedron Lett.* **2012**, *53*, 5223-5226.
36. Karimi, A. R.; Bayat, F. *Tetrahedron Lett.* **2013**, *54*, 45-48.
37. Khosropour, A. R.; Khodaei, M. M.; Moghannian, H. *Synlett* **2005**, 955-958.
38. Riesen, A.; Zehnder, M.; Kaden, T. A. *Helv. Chim. Acta.* **1986**, *69*, 2074-2080.
39. Enkelkamp, H.; Nolte, R. J. M.; *J. Porphyr. Phthalocya.* **2000**, *4*, 454-459.
40. Frisch, M. *Gaussian 90 User's Guide*; Gaussian, Inc.: Pittsburgh, PA, USA, 1991.
41. Dobbs, K. D.; Hehre, W. J. *J. Comput. Chem.* **1987**, *8*, 861-879.
42. Karimi, A. R.; Dalirnasab, Z.; Karimi, M. *Synthesis* **2014**, *46*, 917-922.